JBC Papers in Press. Published on May 17, 2017 as Manuscript M117.777748
The latest version is at http://www.jbc.org/cgi/doi/10.1074/jbc.M117.777748

β-adrenergic induction of lipolysis in hepatocytes is inhibited by ethanol exposure.

Micah B. Schott[1], Karuna Rasineni[3], Shaun G. Weller[1], Ryan J. Schulze[1], Arthur C. Sletten[2], Carol A. Casey[3,4], and Mark A. McNiven[1*]

[1]*Department of Biochemistry and Molecular Biology and the Center for Basic Research in Digestive Diseases, Mayo Clinic, 200 1st St SW, Rochester, MN, 55905, USA*
[2]*Center for Basic Research in Digestive Diseases, Division of Gastroenterology & Hepatology, Mayo Clinic, Rochester, Minnesota.*
[3]*Department of Internal Medicine, University of Nebraska Medical Center, 988090 Nebraska Medical Center, Omaha, NE, 68198, USA*
[3]*Nebraska Western Iowa Health Care System, Research Service, Omaha, NE, 68105, USA*
*Corresponding Author:

To whom correspondence should be addressed: Dr. Mark McNiven, *Department of Biochemistry and Molecular Biology and the Center for Basic Research in Digestive Diseases, Mayo Clinic, 200 1st St SW, Rochester, MN, 55905, USA, Telephone: (507) 284-0683; FAX: (507) 284-2053;* Email: mcniven.mark@mayo.edu

Keywords *(not in title)*: Lipid droplet, fatty liver, GPCR, cAMP, alcohol

ABSTRACT

In liver steatosis (i.e., fatty liver), hepatocytes accumulate many large neutral lipid-storage organelles known as lipid droplets (LDs). LDs are important in the maintenance of energy homeostasis, but the signaling mechanisms that stimulate LD metabolism in hepatocytes are poorly defined. In adipocytes, catecholamines target the β-adrenergic (β-AR)/cAMP pathway to activate cytosolic lipases and induce their recruitment to the LD surface. Therefore, the goal of this study was to determine whether hepatocytes, like adipocytes, also undergo cAMP-mediated lipolysis in response to β-AR stimulation. Using primary rat hepatocytes and human hepatoma cells, we found that treatment with the β-AR agent isoproterenol caused substantial LD loss via activation of cytosolic lipases adipose triglyceride lipase (ATGL) and hormone-sensitive lipase (HSL). β-adrenergic stimulation rapidly activated cAMP-dependent protein kinase (PKA), which led to the phosphorylation of ATGL and HSL and their recruitment to the LD surface. To test whether this β-AR–dependent lipolysis pathway was altered in a model of alcoholic fatty liver, primary hepatocytes from rats fed a 6-week ethanol (EtOH)-containing Lieber-DeCarli diet were treated with cAMP agonists. Compared with controls, EtOH-exposed hepatocytes showed a drastic inhibition in β-AR/cAMP-induced LD breakdown and the phosphorylation of PKA substrates, including HSL. This observation was supported in VA-13 cells, an EtOH-metabolizing human hepatoma cell line, which displayed marked defects in both PKA activation and isoproterenol-induced ATGL translocation to the LD periphery. In summary, these findings suggest that β-AR stimulation mobilizes cytosolic lipases for LD breakdown in hepatocytes, and perturbation of this pathway could be a major consequence of chronic EtOH insult leading to fatty liver.

The liver is an important mediator of fat storage and lipid homeostasis in the body. Hepatocytes, the most abundant cell type of the liver, constitutively regulate their lipid content via import, synthesis, storage, metabolism and secretion of fatty acids in response to a variety of physiological conditions such as nutrient flux or energy expenditure (1). Disruption of this balance can lead to fatty liver disease, an ailment that is often observed in the obese and exacerbated by the over-consumption of alcohol (2-4). Thus, there is a critical clinical need to understand the mechanisms that govern hepatocellular lipid regulation.

Within hepatocytes, fatty acids are packaged as triglycerides (TG) or sterol esters (SE) and stored within specialized organelles known as lipid droplets (LDs). Although once thought to be inert sites of TG storage, LDs are now understood to have widespread metabolic importance and are regulated by a distinct proteome of constitutively and dynamically associated proteins (5-9). In the liver, catabolism of LDs is mediated in part by lipophagy, or the autophagic targeting of LDs for lysosomal degradation (10,11). Indeed, several studies from our lab and others have helped define the role of vesicular trafficking mediators such as Rab GTPases in guiding the interaction of LDs with autophagic membranes as a requirement for LD catabolism under nutrient starvation (12-14). In addition, the large mechanoenzyme dynamin 2 has also been shown to mediate lipophagy by supporting lysosomal integrity (15,16) and is implicated in the scission of Atg9-positive autophagic vesicles (17). In addition to lipophagy, however, many cell types catabolize LDs through the action of cytosolic lipases that interact and function directly on the LD monolayer (18-20). This lipolytic machinery is integral to adipocyte function and is regulated largely by β-adrenergic activation of the cAMP/PKA pathway, leading to phosphorylation of hormone sensitive lipase (HSL) and adipose triglyceride lipase (ATGL) as well as members of the perilipin family of coat proteins that regulate the access of lipases and other regulatory cofactors to the LD (21-24). Although many of these lipolytic proteins are expressed in hepatocytes and are known to be important for hepatic fat content (25-29), the mechanisms that regulate lipolysis in hepatocytes remain poorly defined.

In this study, we tested the hypothesis that hepatocytes, like adipocytes, also utilize a lipolytic machinery that is activated by β-adrenergic stimuli to break down and subsequently catabolize LDs. We report that β-adrenergic stimulation of hepatocytes using the agonist isoproterenol causes LD loss via the cAMP/PKA pathway. This process requires the cytosolic lipases ATGL and HSL which are phosphorylated and trafficked to LDs within 60 minutes of stimulation. Importantly, we find that the activation of this pathway is significantly perturbed in hepatocytes subjected to either chronic or acute ethanol (EtOH) exposure leading to steatotic cells.

RESULTS

β-adrenergic/cAMP stimulation causes LD loss in hepatocytes—We first sought to determine whether LD catabolism is inducible in hepatocytes upon activation of the β-AR/cAMP pathway by testing the effect of cAMP-elevating agents isoproterenol and forskolin on Hep3B hepatoma cells and freshly-isolated primary rat hepatocytes. Isoproterenol is a selective agonist for β-adrenergic (β-AR) receptors, a class of G protein-coupled receptors (GPCRs) that stimulates cAMP elevation through $G\alpha_s$-mediated activation of adenylyl cyclase. Forskolin is a direct and potent activator of adenylyl cyclase and served as a GPCR-independent positive control for cAMP elevation. To test the effect of β-AR stimulation on LD catabolism, Hep3B cells were first loaded with oleic acid (OA, 150μM, 16h) to induce the formation of LDs, then washed and chased in OA-free, full-serum medium (10% FBS) in the presence or absence of the isoproterenol (Iso, 50μM). As seen in confocal images from Fig. 1a-a', isoproterenol-treated cells had a marked reduction in LDs after just 4 hours. Quantification revealed a 33% reduction in total LD area per cell during this time (n=7 experiments, *$p<0.05$). Interestingly, the effect of isoproterenol on Hep3B LDs was selective to larger-sized LDs (>2μm^2) relative to the overall LD population, in which a significant 44% reduction was observed, whereas there was no significant reduction in smaller sized LDs (0-2μm^2, Supplemental Fig. 1a). Similar results were observed in primary rat hepatocytes. Following hepatocyte isolation, cells were equilibrated in regular growth medium (no oleic acid) on collagen-coated glass coverslips for 24 hours before treatment with cAMP agonists. As seen in confocal images and quantification in Fig. 1c-d, isoproterenol caused a 22% reduction in total LD area per cell, and direct cAMP elevation by forskolin + IBMX caused an even more dramatic 48% loss over the course of 24 hours. As observed in the Hep3B cells, the agonist-induced LD loss in primary rat hepatocytes was preferential to relatively larger-sized LDs (>5μM^2), where we observed a 36% and 68% loss by isoproterenol and forskolin + IBMX, respectively (Supplemental Fig. 1b). These data demonstrate that LD breakdown in hepatocytes is inducible by β-AR stimulation, and that cAMP elevation is a potent stimulus for LD catabolism.

β-adrenergic stimulation in hepatocytes activates the cAMP/PKA pathway—Isoproterenol is a widely-used agonist for β-AR stimulation and triggers the canonical activation of protein kinase A (PKA) downstream of cAMP elevation in many cells and tissues. To confirm in our hepatocyte cell models that the cAMP/PKA pathway was indeed being activated by isoproterenol, we used quantitative FRET microscopy and Western blot analysis to establish the potency and time course of PKA activation following treatment. First, we transfected Hep3B cells with the FRET-based PKA biosensor AKAR4, which was targeted to the cytosol by a C-terminal nuclear export sequence (NES). This biosensor has been thoroughly characterized as a highly specific indicator of subcellular PKA activation in live cells and in real time (30). Upon cAMP elevation, activated PKA phosphorylates the AKAR4 biosensor, resulting in a real-time increase in AKAR4 FRET intensity while the CFP donor fluorescence decreases simultaneously and thus can be measured as a ratio of FRET/CFP (Supplemental Fig. 2). As seen in Figure 2, representative ratiometric images depicting FRET/CFP show PKA activity levels before treatment and at 5 min post-treatment with cAMP agonists. At 5 minutes, both 50μM isoproterenol (2a-a') and 10μM forskolin (2c-c') caused a substantial elevation in PKA activity as detected by an increase in the ratio of FRET/CFP. Quantification of this increase showed a 14% increase in PKA activity by isoproterenol (2b) and an even more substantial 45% increase by forskolin (2d). Consistent with this, we also treated primary rat hepatocytes with cAMP-elevating agents to detect the presence of PKA-phosphorylated substrates by Western blot analysis using an antibody raised against a PKA-specific phosphorylated amino acid motif (RRXpS/T). As seen in Fig. 2e, Western blot analysis of cell lysates treated for 1h with either 50μM isoproterenol or 10μM forskolin + 0.5mM IBMX showed an increase in the number and intensity of PKA-phosphorylated substrates. As expected, forskolin was more potent than isoproterenol in its ability to activate PKA, which is consistent with FRET biosensor findings and the relative potency of these agonists to induce LD breakdown in primary rat hepatocytes as was observed in Fig. 1.

β-adrenergic LD breakdown occurs by PKA-dependent activation of cytoplasmic lipases.—Given that isoproterenol activated the cAMP/PKA pathway in our hepatocyte models, we reasoned that this pathway was also responsible for mediating the loss in LD content following stimulation. To test this, we treated primary rat hepatocytes with isoproterenol in the presence and absence of H89, a potent pharmacological agent that inhibits PKA. As seen in figure 3a-a", 50μM isoproterenol treatment for 24 h caused a nearly 40% reduction in LD area per cell in the absence of the inhibitor. ($n=3$, $p<0.05$). However, in the presence of H89, isoproterenol caused no reduction in LD area per cell, suggesting that β-AR stimulation of hepatocytes results in LD loss via the cAMP/PKA pathway.

Based on adipocyte studies, it is well-established that the cAMP/PKA pathway mediates LD breakdown through the process of lipolysis, in which PKA activates and recruits cytosolic lipases ATGL (adipose triglyceride lipase) and HSL (hormone-sensitive lipase) from the cytosol to the LD surface, thus allowing for the hydrolysis of free fatty acids from glycerol and sterol ester backbones (7,20,21,31,32). To test the contribution of the lipolysis pathway in isoproterenol-induced LD breakdown, pre-treatment for 2 h with the ATGL inhibitor atglistatin (10μM, 3c-c") or the HSL inhibitor CAY10499 (10μM, 3d-d") each prevented LD breakdown following isoproterenol treatment (50μM, 24h), suggesting that in addition to PKA activation, cytosolic lipase activity is involved in LD breakdown following β-AR stimulation in hepatocytes. Importantly, both ATGL and HSL are known to be phosphorylated in response to PKA activity, and this stimulates both lipase activation and recruitment to the LD (7,18,20,21,31,32). To test whether ATGL and HSL are phosphorylated downstream of isoproterenol treatment in hepatocytes, we probed their phosphorylation states by Western blot analysis using phospho-specific antibodies. As seen in Fig. 3E, we detected an increase in HSL phosphorylation (S660) in primary rat hepatocytes within 1 hour of isoproterenol treatment. However, pre-treatment with H89 (10μM, 2 hrs) completely blocked isoproterenol-induced HSL phosphorylation, suggesting that β-AR stimulation caused HSL phosphorylation in a PKA-dependent manner. As a positive control, direct cAMP elevation by 10μM forskolin + 0.5mM IBMX resulted in a substantial increase in phosphorylated HSL (Fig. 3E). In agreement with

this, we observed a similar pattern of ATGL phosphorylation in Hep3B cells that were pre-treated overnight with 10μM H89 to reduce basal phospho-ATGL levels, then washed and treated for 4 h with cAMP-elevating agents. As seen in Fig. 3F, 50μM isoproterenol treatment increased ATGL phosphorylation (S404), but this effect was not observed in cells stimulated with isoproterenol in the presence of H89 during the 4 h treatment. In addition, cAMP elevation by forskolin + IBMX also increased ATGL phosphorylation. These data suggest that hepatocyte β-ARs stimulate lipolysis through the PKA-dependent phosphorylation of cytosolic lipases HSL and ATGL.

Cytoplasmic lipases are trafficked to the LD upon β-adrenergic/cAMP stimulation—The process of lipolysis is in large part regulated by the spatial recruitment of lipases from the cytoplasm to the LD surface. To test whether β-AR stimulation in hepatocytes alters the spatial distribution of cytosolic lipases, we examined the effect of forskolin and isoproterenol treatment on ATGL and HSL localization. First, we tested the recruitment of endogenous ATGL to LDs by Western blotting of isolated LDs in Huh-7 human hepatoma cells, a hepatocyte model that is commonly used for isolating hepatocellular LDs due to high levels of baseline LD content (6,13-15,33). As seen in figure 4a-b, ATGL was detected in both the post-nuclear supernatant (PNS) and in isolated LDs under DMSO control conditions. Upon treatment with forskolin (10μM, 1h), we observed a significant 31% increase in LD-enriched ATGL levels relative to Plin2 (n=3, $p<0.05$). To further test the trafficking of ATGL to the LD in real-time, we used live-cell microscopy of Hep3B cells expressing an EGFP-tagged ATGL(S47A) mutant construct. The S47A mutation blocks the fatty-acid hydrolysis activity of ATGL (19), which allowed us to visualize the spatial dynamics of the lipase while avoiding the implicit reduction of LD levels due to overexpression of active ATGL. Importantly, the cAMP-induced spatial dynamics we observed in the S47A mutant were confirmed using WT ATGL-EGFP (Supplemental Movie 1). As seen in Fig. 4c-c', treatment with isoproterenol increased ATGL(S47A)-EGFP intensity around LDs that were labeled with MDH, a LD-specific dye. The redistribution of ATGL from the cytoplasm to the LD was more graphically seen in pseudocolored heatmap images depicting the fluorescence intensity of the EGFP channel (4e-e'), whereby we observed a substantial decrease in cytosolic ATGL intensity (yellow arrows) while ATGL intensity around the LDs simultaneously increased. To quantify these changes across multiple cells, we measured the EGFP fluorescence intensity within regions of interest surrounding several LDs in each cell before isoproterenol treatment and 60 minutes after treatment, normalized to cytosolic EGFP fluorescence intensity at each corresponding time point. The ratios of LD/cytosolic EGFP fluorescence intensity before and after treatment were quantified as a fold change in LD-localized EGFP intensity. This analysis revealed a nearly 2-fold increase in lipase localization around the LD following isoproterenol treatment within 60 minutes (n=10 cells from 3 independent experiments; *$p<0.05$). To test whether direct cAMP elevation had a similar effect, cells treated with 10μM forskolin also showed a significant increase in ATGL(S47A)-EGFP intensity around the LD within 60 minutes, but this effect was blocked by 2-hour pre-treatment with 10μM H89 (n=13-14 cells from 3 independent experiments; *$p<0.05$). We also tested the effects of these agonists on a superfolder GFP (sfGFP)-tagged HSL construct (HSL-sfGFP) expressed in Hep3B cells. As seen in figure 5, isoproterenol caused a ~50% increase in HSL localization around the LD, a more modest redistribution compared to that of ATGL, within just 30 minutes of treatment (n=13 cells from 3 independent experiments; *$p<0.05$). In addition, forskolin treatment caused a similar increase in HSL localization around the LD, but this was blocked by a 2-hour pretreatment with 10μM H89 (n=13-19 cells from 3 independent experiments; *$p<0.05$). These data suggest that β-AR/cAMP activation in hepatocytes triggers cytosolic lipase translocation to the LD and suggests that the mechanism of β-AR mediated LD breakdown in hepatocytes occurs in part through the spatial regulation of cytosolic lipases.

To further test our conclusions that cAMP/PKA signaling regulates the spatial distribution of cytosolic lipases in hepatocytes, we measured the effect of the PKA inhibitor H89 on fluorescence recovery after photobleaching (FRAP) in Hep3B cells expressing ATGL(S47A)-EGFP or HSL-sfGFP within regions of interest around the periphery of the LD. As seen in figure 6a, ATGL FRAP was consistently observed in the

absence of inhibitor over 20 minutes at a recovery rate that closely matches a previous FRAP study of this lipase (34). However, 2-hour pretreatment with 10μM H89 significantly inhibited the magnitude of recovery after photobleaching. To quantify the difference in fluorescence recovery, we calculated the mean plateau, or maximum fold recovery, using software-based nonlinear regression curve-fitting (GraphPad Prism 7.0). Based on these calculations, pretreatment for 2 hours with 10μM H89 caused a ~70% reduction in the fold recovery of ATGL after photobleaching (Fig. 6c). Similarly, FRAP of HSL-sfGFP was also significantly inhibited by H89 pre-treatment (Fig. 6d-e), although to a lesser extent than that of ATGL. Interestingly, the presence of H89 did not significantly reduce the rate of recovery for each lipase (Fig. 6f), but the recovery dynamics of ATGL vs HSL were found to differ considerably under basal conditions. Calculations of half-time recovery (i.e. the time at which each lipase recovered to 50% of plateau) revealed that ATGL recovered approximately 5x more slowly than HSL, which suggests that these lipases utilize different mechanisms for LD recruitment and localization (Fig. 6G). Taken together, these data support the notion that cAMP-dependent signaling regulates lipase localization at the LD, suggesting that these dynamics may be integral to the mechanisms of β-AR/cAMP-induced LD breakdown in hepatocytes.

EtOH exposure inhibits β-adrenergic/cAMP mediated LD loss in hepatocytes—Given our mechanistic understanding of the β-AR lipolysis pathway in hepatocytes, we sought to determine whether this was perturbed under conditions that promote hepatic fat accumulation. To test this, we applied various *in vitro* and *in vivo* models of alcohol consumption, a well-known risk factor for hepatic steatosis, and measured the ability of hepatocytes to degrade LDs in response to cAMP elevation. Using primary rat hepatocytes, we first observed that pretreatment with 50mM EtOH for 24 hours prior to agonist stimulation caused a significant block in LD breakdown by isoproterenol (50μM, 24h), but not by 10μM forskolin + 0.5mM IBMX (Supplemental Fig. 3). To test whether a similar result was observed in a model of chronic alcohol consumption, we isolated primary hepatocytes from rats that were pair-fed either an EtOH-containing Leiber-DeCarli liquid diet or an isocaloric control diet for 6 weeks. As seen in Fig. 7a-b, primary hepatocytes from EtOH-fed rats had roughly 2-fold greater LD area per cell compared with controls. In hepatocytes from control rats, 24h treatment with Iso or Fsk+IBMX resulted in a significant decrease in LD area/cell, however these cAMP-elevating agents caused no reduction in LD content in primary hepatocytes from EtOH-fed rats. Biochemical measurements of triglyceride efflux after 4 hours of treatment with Fsk+IBMX also revealed a significant inhibition of lipolysis in hepatocytes from chronic EtOH-fed rat, a response that was also sensitive to the ATGL inhibitor atglistatin (ASTAT, Fig. 7c). To test whether the chronic EtOH diet altered the activation of cytosolic lipases in response to cAMP/PKA activation, Western blot analysis revealed that in control hepatocytes, treatment with isoproterenol (50μM, 1h) caused a robust phosphorylation of HSL that was sensitive to the PKA inhibitor H89. The phospho-HSL response was even more substantial in cells treated with Fsk+IBMX (Fig. 7d-e). However, in hepatocytes from EtOH-fed rats, phosphorylation of HSL was dramatically reduced following either isoproterenol treatment or Fsk+IBMX (Fig. 7d-e). Western blot analysis revealed that the cAMP synthesis enzyme adenylate cyclase 3, as well as the catalytic subunit of PKA (PKA-Cα), were not significantly reduced in hepatocytes from chronic EtOH-fed rats vs controls (Fig 7f), suggesting that the inhibitory effects of EtOH were not due to a reduction in PKA or cAMP synthesis. To further test whether EtOH inhibition occurred downstream of cAMP synthesis, we treated primary hepatocytes with the cell-permeable cAMP analogue 8-Br-cAMP (10μM, 100μM; 1h) or forskolin+IBMX and analyzed PKA activity by measuring the increase in PKA phospho-substrates, including HSL. As seen in Figure 7g, Western blot analysis revealed that both 8-Br-cAMP and Fsk+IBMX treatment resulted in an increase in the detection of PKA phospho-substrates and phospho-HSL in hepatocytes from control rats, however this increase was greatly reduced in hepatocytes from chronic EtOH-fed rats. Densitometry analysis revealed a remarkable 60-80% reduction in the detection of PKA phospho-substrate (Fig. 7h) and an even more substantial 90% reduction in phosphorylated HSL (Fig. 7i). These data show for the first time that the PKA pathway is a major inhibitory target of chronic

EtOH consumption that inhibits the phosphorylation of many PKA substrates, including HSL, and reduces the catabolism of LDs in response to β-adrenergic/cAMP activation.

EtOH inhibits isoproterenol-induced ATGL recruitment to the LD in VA-13 cells—To test whether EtOH affected cAMP-induced trafficking of cytosolic lipases to the LD, we utilized an EtOH-metabolizing human hepatocyte model, VA-13 cells, for the transient expression of the ATGL(S47A)-EGFP construct. VA-13 cells are a widely-utilized cell model for EtOH studies and are derived from HepG2 human hepatoma cells that stably express alcohol dehydrogenase, or ADH (See Ref. 35, Fig. 8e). Prior to microscopy, cells were pre-treated with or without EtOH (50mM, 48h) and loaded with oleic acid (150μM, 16h). LDs were labeled by 15-minute pre-incubation with MDH. As seen in Figure 8a-b, treatment with 50μM isoproterenol + 0.5mM IBMX resulted in the recruitment of ATGL to the LD surface within 30 minutes in control cells, but ATGL recruitment was blocked in cells pre-treated with EtOH. To confirm that EtOH caused a similar PKA defect as observed in primary hepatocytes from chronic EtOH-fed rats, Western blot analysis using a phospho-PKA substrate antibody revealed a step-wise reduction in PKA phospho-targets that was ~30% reduced by day 2 and more than 50% reduced by day 5. These data suggest that, following β-AR stimulation, PKA activation and cytosolic lipase recruitment to the LD are severely impaired by EtOH.

DISCUSSION

The central findings of this study support the premise that, like the adipocyte, the hepatocyte is responsive to β-AR stimulation that triggers a cAMP-dependent cascade involving cytoplasmic lipases that are recruited to the LD surface to drive lipid catabolism. Unlike the adipocyte, the hepatocyte has the capacity to detoxify EtOH which appears to substantially attenuate this process. We find that the cAMP agonists isoproterenol and forskolin+IBMX, which rapidly activate cAMP-dependent protein kinase, or PKA, lead to a significant catabolic utilization of LDs by both cultured primary hepatocytes and human hepatoma cells **(Fig 1, 2).** This cAMP-induced reduction in total LD content was prevented by the pharmacological PKA inhibitor H89, the ATGL inhibitor atglistatin, and the HSL inhibitor CAY10499. β-adrenergic stimulation resulted in the phosphorylation of HSL and ATGL, both of which were mimicked by Fsk+IBMX treatment and blocked by inhibition with H89 **(Fig. 3).** cAMP elevation also triggered the recruitment of these lipases from the cytoplasm to the LD surface in Hep3B cells **(Fig. 4, 5)**. To our knowledge, this study is the first to compare these two activated lipases in terms of their dynamics and recruitment to the LD surface, and this approach provided some new insights. First, even under basal or "resting" conditions, protein exchange of LD-localized ATGL was slower than that of HSL, which displayed a half-time recovery of 1.3 minutes as opposed to 6.5 minutes for ATGL as determined by FRAP studies. Further, the recruitment of each lipase was significantly reduced by the inhibitor H89, which supports our notion that PKA is an important determinant of lipase localization in hepatocytes. **(Fig. 6)**. Finally, chronic EtOH exposure in primary rat hepatocytes blocked cAMP-induced LD breakdown and caused a dramatic decrease in the phosphorylation of PKA substrates, including HSL. **(Fig. 7)**. Live-cell microscopy of VA-13 cells, an ethanol-metabolizing hepatocyte cell model, further reveled that ethanol exposure perturbs the recruitment of ATGL to the LD following β-AR/cAMP stimulation. Western blot analysis revealed a substantial reduction in PKA phospho-substrates in the presence of EtOH. **(Fig. 8)**. These findings indicate that activation of hepatocellular β-ARs can stimulate LD breakdown through cytosolic lipases, and that the β-AR/cAMP/lipolysis pathway appears to be exceptionally sensitive to EtOH exposure.

The cAMP pathway: a central regulator of energy homeostasis—cAMP signaling in hepatocytes has been predominantly attributed to glucose production in response to the hormone glucagon, a GPCR ligand that targets hepatocytes under conditions of low blood glucose (1). Glucagon targets hepatocellular glucagon receptors to elevate cAMP and stimulate gluconeogenesis and glycogenolysis (1,36,37). In addition to glucose production, several past studies have demonstrated that the glucagon/cAMP pathway also induces hepatic lipid metabolism through an autophagic/lysosomal pathway (Reviewed in 11), a process more recently termed "lipophagy" (10). Although lipophagy has been demonstrated as an

important mechanism for hepatic lipid clearance, our study suggests that an adipocyte-like lipolysis mechanism also governs hepatic lipid content via β-AR stimulation of hepatocytes.

From the current study, the effects of β-AR stimulation on LD breakdown through cytosolic lipases ATGL and HSL provide mechanistic insight that complements previous work from other laboratories. Mashek and colleagues were first to show that ATGL is a major regulator of triglyceride content in hepatocytes by activating the Sirt1/PGC-1α/PPARα transcriptional axis (25,38). Recently, ATGL activation of Sirt1 was shown to play an important role in the transcriptional activation of autophagy leading to fatty acid turnover in mouse hepatocytes, further substantiating the role of cytosolic lipases in regulating hepatic lipid turnover. HSL, on the other hand, was previously regarded as absent from the liver based on antibody staining (39), but later studies demonstrated that knockout or inhibition of HSL reduced triglyceride hydrolase activity and FFA levels in cell extracts from mouse livers (40,41). In addition, Sekiya et al. (2008) proposed that HSL is important for hydrolysis of cholesterol esters in hepatocytes (42). Our current study supports these findings and further suggests that both ATGL and HSL are stimulated by the cAMP pathway for LD catabolism in hepatocytes, much like in adipocytes. Both of these lipases were phosphorylated following β-AR stimulation and were measurably recruited to the LD within 1 hour of stimulation, and pharmacological inhibitors against each lipase blocked β-AR induced LD clearance. The adipocyte-like response of these lipases in hepatocytes is somewhat surprising, as the two cell types are reported to express different perilipin members that regulate the access of lipases and other accessory proteins to the LD surface (43). For example, the LD-associated protein perilipin (PLIN1) is predominant in adipocytes and largely absent in hepatocytes under normal conditions, and yet PLIN1 phosphorylation is critical for HSL recruitment to the LD (23,44). Thus, HSL may interact with other hepatocyte-centric perilipin members to mediate LD recruitment (i.e. PLIN2, PLIN3, PLIN5). Future work will be required to dissect the precise mechanisms regulating hepatocellular lipase activity and access to the LD, including the accessory proteins behind this response.

Although our studies demonstrate a role for cytoplasmic lipases in cAMP-induced hepatic lipid clearance, the role of lipophagy upon β-AR stimulation requires further investigation. Several lines of evidence link cAMP elevation to induction of autophagy in hepatocytes. First, Farah et al. (2014) demonstrate that β-AR agonists induce LC3-II formation and p62 degradation in primary mouse hepatocytes and human hepatoma cells (45). Another study showed that caffeine, an adenosine receptor antagonist and phosphodiesterase inhibitor, stimulates lipid metabolism and autophagy (LC3-II increase and p62 decrease), as well as suppresses mTORC1 activity (46). Although the role of autophagy was not investigated in the current study, it is likely that β-adrenergic stimuli also utilize lipophagy as a downstream consequence of the cAMP/lipolysis pathway in hepatocytes, possibly through a transcriptionally-regulated response (38,47,48).

The *in vivo* contribution of β-adrenergic signaling in the clearance of hepatocellular lipid droplets is currently unclear. Circulating catecholamines are known to activate lipolysis in peripheral tissues such as adipose and skeletal muscle that release fatty acids that are taken up by the liver, causing acute hepatic steatosis (49). Given the results from our current study, we predict that hepatocytes utilize the β-adrenergic lipolysis pathway *in vivo* to counterbalance the acute influx of fat from peripheral tissues and mediate the subsequent clearance of LDs following epinephrine-release during exercise, fasting, or a "fight-or-flight" response. This notion is supported by a recent systematic review that highlighted the role of exercise on improving non-alcoholic fatty liver disease (NAFLD), suggesting that circulating catecholamines may play an important long-term role in reducing fat accumulation in the liver (50). Other studies have shown that hepatic β-adrenergic levels increase during senescent aging, which unexpectedly correlates with a higher incidence of hepatic steatosis (49,51,52). It is important to note that aging also diminishes hepatic mitochondrial functions including fatty acid oxidation (53), and aging has been associated with a decrease in ATGL levels in muscle (54). Although the current study predicts a possible therapeutic role of β-adrenergic signaling in hepatic lipid droplet clearance, further studies will be required to fully understand how

downstream lipolytic mediators are regulated in both young and aged individuals.

Inhibition of hepatocyte LD breakdown by EtOH exposure-implications in hepatic steatosis—The impact of EtOH on fat accumulation in the liver has long been appreciated as it leads to the accumulation of hepatocellular NADH, an excess of which inhibits pyruvate formation and fatty acid oxidation, thus increasing fatty acid synthesis (3). In addition to this, our current study demonstrates that LD breakdown by hepatic lipolysis is also inhibited by EtOH insult. Both acute and chronic EtOH exposure completely blocked isoproterenol-induced LD breakdown in primary rat hepatocytes. Interestingly, acute EtOH exposure did not prevent LD breakdown by direct cAMP agonists Fsk+IBMX, which points to possible differences between acute vs chronic EtOH insult with regard to inhibiting LD breakdown. It is possible that highly-potent Fsk+IBMX treatment was able to overcome the inhibitory effects of acute EtOH exposure. Ethanol is known to disrupt β-adrenergic receptor-ligand affinity in other tissues such as the brain and heart (55), however our chronic EtOH model suggests that the inhibition of lipolysis lies downstream of receptor-ligand binding and cAMP synthesis. As shown in Fig. 7, the cell-permeable cAMP analogue 8-Br-cAMP caused an increase in PKA phospho-targets in control hepatocytes, but this was greatly reduced in hepatocytes from EtOH-fed rats. To our knowledge, this is the first report indicating that EtOH inhibits the cAMP/PKA pathway in hepatocytes, although similar phenomena have been reported to occur in other non-EtOH metabolizing tissues (56,57). This finding could provide insights into a variety of detrimental effects that EtOH has on hepatocellular functions such as gluconeogenesis, as hypoglycemia is one of the hallmarks of excessive alcohol consumption (58). The mechanism by which EtOH inhibits cAMP/PKA signaling is currently unclear and requires further investigation, but an attractive possibility could involve the activation of protein phosphatases by ceremide, a cellular byproduct of EtOH metabolism or high-fat diet (59-64).

In conclusion, our observations from primary rat hepatocytes and human hepatoma cell lines together suggest that the β-adrenergic receptor mediate hepatocellular lipid catabolism by activating the cAMP/PKA pathway. This pathway leads to phosphorylation of the cytosolic lipases ATGL and HSL and rapidly mobilizes these lipases to the LD surface. These events are perturbed by EtOH insult, which inhibits LD breakdown and the phosphorylation of PKA substrates including hormone sensitive lipase, as well as inhibits the recruitment of adipose triglyceride lipase to the LD periphery. Based on these results, it is possible that chronic alcohol consumption blocks LD catabolism through the inhibition of the PKA pathway, which represents a novel mechanism in the pathogenesis of fatty liver disease

EXPERIMENTAL PRODECURES

Cell culture and reagents—Primary rat hepatocytes were isolated from female Sprague Dawley rats (Envigo) by collagenase perfusion and were cultured in William's E Medium (5% FBS) as described by Shen et al. (65). For experiments involving chronic EtOH diet, male Wistar rats (Charles River Labs, Portage MI) were paired according to weight (175-200 g) and fed control and EtOH-containing Lieber-DeCarli diets (66) for 5-8 weeks as previously described (67). All animals received humane care in accordance with the guidelines established by the American Association for the Accreditation of Laboratory Animal Care. All protocols were approved by the Institutional Animal Care and Use Committee at Mayo Clinic and the VA NWIHCS Research Service. The Hep3B2.1-7 (Hep3B) human hepatoma cell line was obtained from ATCC (HB-8064) and maintained in complete MEM (10% FBS, Pen/Strep, minimal essential amino acids, $NaHCO_3$, and sodium pyruvate). VA-13 cells and the alcohol dehydrogenase (ADH) antibody were gifts from Dr. Terrence Donahue (UNMC and the Dept. of Veterans' Affairs, Omaha, NE). VA-13 cells are human HepG2 hepatoma cells that stably express ADH and thus metabolize EtOH in culture (35). VA-13 cells were maintained in DMEM with 10% FBS, Pen/Strep, and 1:250 zeocin (Invitrogen #R25001, 100mg/ml). The β-actin antibody (#A2066), Oil Red O (#O0625), isoproterenol (I2760), forskolin (F6886), IBMX (I7018) and H89 (B1427) were from Sigma. The phospho-PKA substrate antibody (#9624), phospho-HSL (Ser660) antibody (#4126), and ATGL antibody (#2138) were from Cell Signaling Technology. The Plin2 antibody (#B3121) was from LS Biosciences. The HSL antibody (AB45422) was from Abcam. The

phospho-ATGL (S404) antibody (31) was a gift from Dr. Matthew Watt (Monash University). The ATGL inhibitor atglistatin (#15284) and the HSL inhibitor CAY10499 (CAS #359714-55-9) were from Cayman Chemical. The MDH LD dye was from Abgent (SM1000a).

Triglyceride efflux measurements—Primary hepatocytes from control and EtOH-fed rats were cultured as previously described (67). Upon isolation, cells were suspended William's E medium and seeded onto collagen-coated 6-well plates. After 2 h at 37°C, cells were washed and treated an additional 4 h in Williams medium with 5% FBS containing DMSO, 10μM forskolin + 0.5mM IBMX, 10μM atglistatin, or Fsk+IBMX+atglistatin. Cells were then pelleted and reconstituted in PBS. Triglyceride extraction was done according to Folch *et al*. (68). Aliquots of lipid extract were saponified and assessed using a triglyceride diagnostic kit (Thermo DMA kit, Thermo Electron Clinical Chemistry, Louisville, CO). Triglyceride levels were normalized to total DNA content and quantified as the percent loss from the initial TG value as previously described (69).

Constructs and transfection—The PKA FRET biosensor pcDNA3-AKAR4-NES was a gift from Jin Zhang (Addgene plasmid # 64727) (30). The human ATGL-EGFP and catalytically inactive ATGL(S47A)-EGFP constructs were gifts from Dr. Cathy Jackson (Institut Jacques Monod, Paris). We generated the HSL-sfGFP construct from a mouse HSL-FLAG plasmid received as a gift from Dr. Jun Liu (Mayo Clinic, AZ). A PCR product containing the HSL sequence was cloned into a superfolder GFP construct at SacII and HindIII restriction sites (forward primer: 5'-AGAAAGCTTGAATTGATGGAG; reverse primer – 5' – AAAACCGCGGGTTCAGTGGT) and confirmed by sequence analysis.

Fluorescence microscopy—Cells were washed in PBS and fixed in 3% formaldehyde as described previously. To label LDs, fixed samples were washed in 60% isopropanol for 30 seconds, 60% Oil Red O solution (5mg/ml in isopropanol) for 2.5 minutes, then washed in 60% isopropanol for an additional 30 seconds. Images were acquired using a Zeiss LSM 780 confocal microscope with a 40x oil objective lens (NA=1.4). LD measurements were done using ImageJ software. Images of LDs were first made binary using the auto local threshold tool (Bernsen method), and LD area and number was quantified using the analyze particles tool.

Live-cell and FRET imaging—Live-cell imaging was performed on a Zeiss LSM 780 confocal microscope with a 63x water objective lens (NA=1.2) with heated stage incubation (37°C, 5% CO_2). To image the AKAR4 FRET biosensor, cells were excited with a 458nm laser, and two emission channels were simultaneously captured on a spectral detector (CFP emission: 470-500nm; FRET emission: 520-590nm). CFP crossover into the FRET channel was calculated using a single CFP construct and was subtracted for each acquisition (39% of the CFP emission).

Lipid droplet isolation—Isolation of LDs was adapted from Brasaemle and Wollins (70). In brief, Huh7 human hepatoma cells were grown to near-confluency in five 15 cm dishes. Cells were lysed using a Dounce homogenizer, and the post-nuclear supernatant (PNS) was placed at the bottom of a 30% to 0% OptiPrep™ density gradient (Sigma D1556). Following a 30 min 17200 rpm spin, the floating fat layer was collected and washed for subsequent Western blot analysis.

Acknowledgements: We are grateful to the members of the McNiven and Casey laboratories for helpful discussion. This work was supported by National Institutes of Health Grants 5R37DK044650 (to M.A.M.), 5RO1AA020735 (to M.A.M. and C.A.C.), 5T32DK007352 (to R.J.S. and M.B.S.), the Department of Veterans' Affairs (C.A.C), and the Optical Morphology Core of the Mayo Clinic Center for Cell Signaling in Gastroenterology (NIDDK P30DK084567). The content is solely the responsibility of the authors and does not necessarily represent the official views of the National Institutes of Health.

Conflict of interest: The authors declare that they have no conflicts of interest with the contents of this article.

Author contributions: M. B. S., K. R., S. W., and R.S contributed to conception, design, acquisition, analysis, and interpretation of data. M.B.S and M.A.M wrote the manuscript, and all authors reviewed the results and approved the final version.

References

1. Rui, L. (2014) Energy metabolism in the liver. *Compr Physiol* **4**, 177-197
2. O'Shea, R. S., Dasarathy, S., and McCullough, A. J. (2010) Alcoholic liver disease. *Am J Gastroenterol* **105**, 14-32; quiz 33
3. Lieber, C. S. (2004) Alcoholic fatty liver: its pathogenesis and mechanism of progression to inflammation and fibrosis. *Alcohol* **34**, 9-19
4. Dam-Larsen, S., Franzmann, M., Andersen, I. B., Christoffersen, P., Jensen, L. B., Sorensen, T. I., Becker, U., and Bendtsen, F. (2004) Long term prognosis of fatty liver: risk of chronic liver disease and death. *Gut* **53**, 750-755
5. Guo, Y., Cordes, K. R., Farese, R. V., Jr., and Walther, T. C. (2009) Lipid droplets at a glance. *J Cell Sci* **122**, 749-752
6. Fujimoto, Y., Itabe, H., Sakai, J., Makita, M., Noda, J., Mori, M., Higashi, Y., Kojima, S., and Takano, T. (2004) Identification of major proteins in the lipid droplet-enriched fraction isolated from the human hepatocyte cell line HuH7. *Biochimica et biophysica acta* **1644**, 47-59
7. Brasaemle, D. L., Dolios, G., Shapiro, L., and Wang, R. (2004) Proteomic analysis of proteins associated with lipid droplets of basal and lipolytically stimulated 3T3-L1 adipocytes. *J Biol Chem* **279**, 46835-46842
8. Cermelli, S., Guo, Y., Gross, S. P., and Welte, M. A. (2006) The lipid-droplet proteome reveals that droplets are a protein-storage depot. *Curr Biol* **16**, 1783-1795
9. Walther, T. C., and Farese, R. V., Jr. (2012) Lipid droplets and cellular lipid metabolism. *Annual review of biochemistry* **81**, 687-714
10. Singh, R., Kaushik, S., Wang, Y., Xiang, Y., Novak, I., Komatsu, M., Tanaka, K., Cuervo, A. M., and Czaja, M. J. (2009) Autophagy regulates lipid metabolism. *Nature* **458**, 1131-1135
11. Debeer, L. J., Beynen, A. C., Mannaerts, G. P., and Geelen, M. J. (1982) Lipolysis of hepatic triacylglycerol stores. *FEBS Lett* **140**, 159-164
12. Rasineni, K., McVicker, B. L., Tuma, D. J., McNiven, M. A., and Casey, C. A. (2014) Rab GTPases associate with isolated lipid droplets (LDs) and show altered content after ethanol administration: potential role in alcohol-impaired LD metabolism. *Alcoholism, clinical and experimental research* **38**, 327-335
13. Schroeder, B., Schulze, R. J., Weller, S. G., Sletten, A. C., Casey, C. A., and McNiven, M. A. (2015) The small GTPase Rab7 as a central regulator of hepatocellular lipophagy. *Hepatology* **61**, 1896-1907
14. Li, Z., Schulze, R. J., Weller, S. G., Krueger, E. W., Schott, M. B., Zhang, X., Casey, C. A., Liu, J., Stockli, J., James, D. E., and McNiven, M. A. (2016) A novel Rab10-EHBP1-EHD2 complex essential for the autophagic engulfment of lipid droplets. *Sci Adv* **2**, e1601470
15. Schulze, R. J., Weller, S. G., Schroeder, B., Krueger, E. W., Chi, S., Casey, C. A., and McNiven, M. A. (2013) Lipid droplet breakdown requires dynamin 2 for vesiculation of autolysosomal tubules in hepatocytes. *J Cell Biol* **203**, 315-326
16. Schulze, R. J., and McNiven, M. A. (2014) A well-oiled machine: DNM2/dynamin 2 helps keep hepatocyte lipophagy running smoothly. *Autophagy* **10**, 388-389
17. Takahashi, Y., Tsotakos, N., Liu, Y., Young, M. M., Serfass, J., Tang, Z., Abraham, T., and Wang, H. G. (2016) The Bif-1-Dynamin 2 membrane fission machinery regulates

Atg9-containing vesicle generation at the Rab11-positive reservoirs. *Oncotarget* **7**, 20855-20868
18. Egan, J. J., Greenberg, A. S., Chang, M. K., Wek, S. A., Moos, M. C., Jr., and Londos, C. (1992) Mechanism of hormone-stimulated lipolysis in adipocytes: translocation of hormone-sensitive lipase to the lipid storage droplet. *Proc Natl Acad Sci U S A* **89**, 8537-8541
19. Smirnova, E., Goldberg, E. B., Makarova, K. S., Lin, L., Brown, W. J., and Jackson, C. L. (2006) ATGL has a key role in lipid droplet/adiposome degradation in mammalian cells. *EMBO Rep* **7**, 106-113
20. Bezaire, V., Mairal, A., Ribet, C., Lefort, C., Girousse, A., Jocken, J., Laurencikiene, J., Anesia, R., Rodriguez, A. M., Ryden, M., Stenson, B. M., Dani, C., Ailhaud, G., Arner, P., and Langin, D. (2009) Contribution of adipose triglyceride lipase and hormone-sensitive lipase to lipolysis in hMADS adipocytes. *J Biol Chem* **284**, 18282-18291
21. Brasaemle, D. L., Levin, D. M., Adler-Wailes, D. C., and Londos, C. (2000) The lipolytic stimulation of 3T3-L1 adipocytes promotes the translocation of hormone-sensitive lipase to the surfaces of lipid storage droplets. *Biochimica et biophysica acta* **1483**, 251-262
22. Granneman, J. G., Moore, H. P., Krishnamoorthy, R., and Rathod, M. (2009) Perilipin controls lipolysis by regulating the interactions of AB-hydrolase containing 5 (Abhd5) and adipose triglyceride lipase (Atgl). *J Biol Chem* **284**, 34538-34544
23. Wang, H., Hu, L., Dalen, K., Dorward, H., Marcinkiewicz, A., Russell, D., Gong, D., Londos, C., Yamaguchi, T., Holm, C., Rizzo, M. A., Brasaemle, D., and Sztalryd, C. (2009) Activation of hormone-sensitive lipase requires two steps, protein phosphorylation and binding to the PAT-1 domain of lipid droplet coat proteins. *J Biol Chem* **284**, 32116-32125
24. Granneman, J. G., Moore, H. P., Mottillo, E. P., Zhu, Z., and Zhou, L. (2011) Interactions of perilipin-5 (Plin5) with adipose triglyceride lipase. *J Biol Chem* **286**, 5126-5135
25. Ong, K. T., Mashek, M. T., Bu, S. Y., Greenberg, A. S., and Mashek, D. G. (2011) Adipose triglyceride lipase is a major hepatic lipase that regulates triacylglycerol turnover and fatty acid signaling and partitioning. *Hepatology* **53**, 116-126
26. Ong, K. T., Mashek, M. T., Bu, S. Y., and Mashek, D. G. (2013) Hepatic ATGL knockdown uncouples glucose intolerance from liver TAG accumulation. *FASEB J* **27**, 313-321
27. Wang, Y., Zhang, Y., Qian, H., Lu, J., Zhang, Z., Min, X., Lang, M., Yang, H., Wang, N., and Zhang, P. (2013) The g0/g1 switch gene 2 is an important regulator of hepatic triglyceride metabolism. *PLoS One* **8**, e72315
28. Carr, R. M., Peralta, G., Yin, X., and Ahima, R. S. (2014) Absence of perilipin 2 prevents hepatic steatosis, glucose intolerance and ceramide accumulation in alcohol-fed mice. *PLoS One* **9**, e97118
29. Wang, C., Zhao, Y., Gao, X., Li, L., Yuan, Y., Liu, F., Zhang, L., Wu, J., Hu, P., Zhang, X., Gu, Y., Xu, Y., Wang, Z., Li, Z., Zhang, H., and Ye, J. (2015) Perilipin 5 improves hepatic lipotoxicity by inhibiting lipolysis. *Hepatology* **61**, 870-882
30. Depry, C., Allen, M. D., and Zhang, J. (2011) Visualization of PKA activity in plasma membrane microdomains. *Mol Biosyst* **7**, 52-58
31. Pagnon, J., Matzaris, M., Stark, R., Meex, R. C., Macaulay, S. L., Brown, W., O'Brien, P. E., Tiganis, T., and Watt, M. J. (2012) Identification and functional characterization of

protein kinase A phosphorylation sites in the major lipolytic protein, adipose triglyceride lipase. *Endocrinology* **153**, 4278-4289
32. Yang, X., Lu, X., Lombes, M., Rha, G. B., Chi, Y. I., Guerin, T. M., Smart, E. J., and Liu, J. (2010) The G(0)/G(1) switch gene 2 regulates adipose lipolysis through association with adipose triglyceride lipase. *Cell Metab* **11**, 194-205
33. Zhang, S., Wang, Y., Cui, L., Deng, Y., Xu, S., Yu, J., Cichello, S., Serrero, G., Ying, Y., and Liu, P. (2016) Morphologically and Functionally Distinct Lipid Droplet Subpopulations. *Sci Rep* **6**, 29539
34. Soni, K. G., Mardones, G. A., Sougrat, R., Smirnova, E., Jackson, C. L., and Bonifacino, J. S. (2009) Coatomer-dependent protein delivery to lipid droplets. *J Cell Sci* **122**, 1834-1841
35. Clemens, D. L., Forman, A., Jerrells, T. R., Sorrell, M. F., and Tuma, D. J. (2002) Relationship between acetaldehyde levels and cell survival in ethanol-metabolizing hepatoma cells. *Hepatology* **35**, 1196-1204
36. Pilkis, S. J., Claus, T. H., Kurland, I. J., and Lange, A. J. (1995) 6-Phosphofructo-2-kinase/fructose-2,6-bisphosphatase: a metabolic signaling enzyme. *Annual review of biochemistry* **64**, 799-835
37. Herzig, S., Long, F., Jhala, U. S., Hedrick, S., Quinn, R., Bauer, A., Rudolph, D., Schutz, G., Yoon, C., Puigserver, P., Spiegelman, B., and Montminy, M. (2001) CREB regulates hepatic gluconeogenesis through the coactivator PGC-1. *Nature* **413**, 179-183
38. Khan, S. A., Sathyanarayan, A., Mashek, M. T., Ong, K. T., Wollaston-Hayden, E. E., and Mashek, D. G. (2015) ATGL-catalyzed lipolysis regulates SIRT1 to control PGC-1alpha/PPAR-alpha signaling. *Diabetes* **64**, 418-426
39. Holm, C., Belfrage, P., and Fredrikson, G. (1987) Immunological evidence for the presence of hormone-sensitive lipase in rat tissues other than adipose tissue. *Biochem Biophys Res Commun* **148**, 99-105
40. Reid, B. N., Ables, G. P., Otlivanchik, O. A., Schoiswohl, G., Zechner, R., Blaner, W. S., Goldberg, I. J., Schwabe, R. F., Chua, S. C., Jr., and Huang, L. S. (2008) Hepatic overexpression of hormone-sensitive lipase and adipose triglyceride lipase promotes fatty acid oxidation, stimulates direct release of free fatty acids, and ameliorates steatosis. *J Biol Chem* **283**, 13087-13099
41. Haemmerle, G., Zimmermann, R., Hayn, M., Theussl, C., Waeg, G., Wagner, E., Sattler, W., Magin, T. M., Wagner, E. F., and Zechner, R. (2002) Hormone-sensitive lipase deficiency in mice causes diglyceride accumulation in adipose tissue, muscle, and testis. *J Biol Chem* **277**, 4806-4815
42. Sekiya, M., Osuga, J., Yahagi, N., Okazaki, H., Tamura, Y., Igarashi, M., Takase, S., Harada, K., Okazaki, S., Iizuka, Y., Ohashi, K., Yagyu, H., Okazaki, M., Gotoda, T., Nagai, R., Kadowaki, T., Shimano, H., Yamada, N., and Ishibashi, S. (2008) Hormone-sensitive lipase is involved in hepatic cholesteryl ester hydrolysis. *Journal of lipid research* **49**, 1829-1838
43. Bickel, P. E., Tansey, J. T., and Welte, M. A. (2009) PAT proteins, an ancient family of lipid droplet proteins that regulate cellular lipid stores. *Biochimica et biophysica acta* **1791**, 419-440
44. Straub, B. K., Stoeffel, P., Heid, H., Zimbelmann, R., and Schirmacher, P. (2008) Differential pattern of lipid droplet-associated proteins and de novo perilipin expression in hepatocyte steatogenesis. *Hepatology* **47**, 1936-1946

45. Farah, B. L., Sinha, R. A., Wu, Y., Singh, B. K., Zhou, J., Bay, B. H., and Yen, P. M. (2014) beta-Adrenergic agonist and antagonist regulation of autophagy in HepG2 cells, primary mouse hepatocytes, and mouse liver. *PLoS One* **9**, e98155
46. Sinha, R. A., Farah, B. L., Singh, B. K., Siddique, M. M., Li, Y., Wu, Y., Ilkayeva, O. R., Gooding, J., Ching, J., Zhou, J., Martinez, L., Xie, S., Bay, B. H., Summers, S. A., Newgard, C. B., and Yen, P. M. (2014) Caffeine stimulates hepatic lipid metabolism by the autophagy-lysosomal pathway in mice. *Hepatology* **59**, 1366-1380
47. Lizaso, A., Tan, K. T., and Lee, Y. H. (2013) beta-adrenergic receptor-stimulated lipolysis requires the RAB7-mediated autolysosomal lipid degradation. *Autophagy* **9**, 1228-1243
48. Sathyanarayan, A., Mashek, M. T., and Mashek, D. G. (2017) ATGL Promotes Autophagy/Lipophagy via SIRT1 to Control Hepatic Lipid Droplet Catabolism. *Cell reports* **19**, 1-9
49. Ghosh, P. M., Shu, Z. J., Zhu, B., Lu, Z., Ikeno, Y., Barnes, J. L., Yeh, C. K., Zhang, B. X., Katz, M. S., and Kamat, A. (2012) Role of beta-adrenergic receptors in regulation of hepatic fat accumulation during aging. *J Endocrinol* **213**, 251-261
50. Whitsett, M., and VanWagner, L. B. (2015) Physical activity as a treatment of non-alcoholic fatty liver disease: A systematic review. *World J Hepatol* **7**, 2041-2052
51. Morgan, N. G., Blackmore, P. F., and Exton, J. H. (1983) Age-related changes in the control of hepatic cyclic AMP levels by alpha 1- and beta 2-adrenergic receptors in male rats. *J Biol Chem* **258**, 5103-5109
52. Katz, M. S., Dax, E. M., and Gregerman, R. I. (1993) Beta adrenergic regulation of rat liver glycogenolysis during aging. *Exp Gerontol* **28**, 329-340
53. Houtkooper, R. H., Argmann, C., Houten, S. M., Canto, C., Jeninga, E. H., Andreux, P. A., Thomas, C., Doenlen, R., Schoonjans, K., and Auwerx, J. (2011) The metabolic footprint of aging in mice. *Sci Rep* **1**, 134
54. Aquilano, K., Baldelli, S., La Barbera, L., Lettieri Barbato, D., Tatulli, G., and Ciriolo, M. R. (2016) Adipose triglyceride lipase decrement affects skeletal muscle homeostasis during aging through FAs-PPARalpha-PGC-1alpha antioxidant response. *Oncotarget* **7**, 23019-23032
55. Hoffman, P. L., Valverius, P., Kwast, M., and Tabakoff, B. (1987) Comparison of the effects of ethanol on beta-adrenergic receptors in heart and brain. *Alcohol Alcohol Suppl* **1**, 749-754
56. De, A., Boyadjieva, N. I., and Sarkar, D. K. (1999) Effects of ethanol on alpha-adrenergic and beta-adrenergic agonist-stimulated beta-endorphin release and cAMP production in hypothalamic cells in primary cultures. *Alcoholism, clinical and experimental research* **23**, 46-51
57. Nagy, L. E., Diamond, I., and Gordon, A. (1988) Cultured lymphocytes from alcoholic subjects have altered cAMP signal transduction. *Proc Natl Acad Sci U S A* **85**, 6973-6976
58. Krebs, H. A., Freedland, R. A., Hems, R., and Stubbs, M. (1969) Inhibition of hepatic gluconeogenesis by ethanol. *Biochem J* **112**, 117-124
59. Wu, Y., Song, P., Xu, J., Zhang, M., and Zou, M. H. (2007) Activation of protein phosphatase 2A by palmitate inhibits AMP-activated protein kinase. *J Biol Chem* **282**, 9777-9788

60. You, M., Matsumoto, M., Pacold, C. M., Cho, W. K., and Crabb, D. W. (2004) The role of AMP-activated protein kinase in the action of ethanol in the liver. *Gastroenterology* **127**, 1798-1808
61. Liangpunsakul, S., Sozio, M. S., Shin, E., Zhao, Z., Xu, Y., Ross, R. A., Zeng, Y., and Crabb, D. W. (2010) Inhibitory effect of ethanol on AMPK phosphorylation is mediated in part through elevated ceramide levels. *American journal of physiology. Gastrointestinal and liver physiology* **298**, G1004-1012
62. Pagadala, M., Kasumov, T., McCullough, A. J., Zein, N. N., and Kirwan, J. P. (2012) Role of ceramides in nonalcoholic fatty liver disease. *Trends in endocrinology and metabolism: TEM* **23**, 365-371
63. Oaks, J., and Ogretmen, B. (2014) Regulation of PP2A by Sphingolipid Metabolism and Signaling. *Front Oncol* **4**, 388
64. Ganesan, M., Zhang, J., Bronich, T., Poluektova, L. I., Donohue, T. M., Jr., Tuma, D. J., Kharbanda, K. K., and Osna, N. A. (2015) Acetaldehyde accelerates HCV-induced impairment of innate immunity by suppressing methylation reactions in liver cells. *American journal of physiology. Gastrointestinal and liver physiology* **309**, G566-577
65. Shen, L., Hillebrand, A., Wang, D. Q., and Liu, M. (2012) Isolation and primary culture of rat hepatic cells. *J Vis Exp*
66. Lieber, C. S., and DeCarli, L. M. (1989) Liquid diet technique of ethanol administration: 1989 update. *Alcohol Alcohol* **24**, 197-211
67. Casey, C. A., McVicker, B. L., Donohue, T. M., Jr., McFarland, M. A., Wiegert, R. L., and Nanji, A. A. (2004) Liver asialoglycoprotein receptor levels correlate with severity of alcoholic liver damage in rats. *J Appl Physiol (1985)* **96**, 76-80
68. Folch, J., Lees, M., and Sloane Stanley, G. H. (1957) A simple method for the isolation and purification of total lipides from animal tissues. *J Biol Chem* **226**, 497-509
69. McVicker, B. L., Rasineni, K., Tuma, D. J., McNiven, M. A., and Casey, C. A. (2012) Lipid droplet accumulation and impaired fat efflux in polarized hepatic cells: consequences of ethanol metabolism. *International journal of hepatology* **2012**, 978136
70. Brasaemle, D. L., and Wolins, N. E. (2016) Isolation of Lipid Droplets from Cells by Density Gradient Centrifugation. *Curr Protoc Cell Biol* **72**, 3 15 11-13 15 13

FIGURE LEGENDS

Figure 1: *LD content is reduced in hepatocytes by β-adrenergic/cAMP agonists.* (A) Confocal micrographs of oleate-loaded Hep3B cells stained for LDs with Oil Red O (ORO) following no treatment (control) or treatment with 50μM isoproterenol for 4h. (B) Corresponding graph shows quantification of the total LD area per cell revealing a 33% agonist-induced reduction (n=7 experiments, p=0.003, Students T-test) (C) Confocal micrographs of ORO-stained LDs in primary rat hepatocytes untreated (control) or treated with 50μM isoproterenol or 10μM forskolin + 0.5mM IBMX for 24h. (D) Corresponding graph shows quantification of the fold difference in total LD area per cell leading to a 21% and 43% reduction, respectively, following stimulation (isoproterenol: n=7 experiments, p=0.034 vs CT; Fsk+IBMX: n=5 experiments, p=0.008, paired T-test vs CT). Dashed circles denote nuclei position in confocal images.

Figure 2: *PKA is activated in hepatocytes by β-adrenergic/cAMP stimulation.* Pseudocolored ratiometric images of Hep3B cells expressing the FRET PKA biosensor AKAR4-NES before and 5 minutes after treatment with 50μM isoproterenol (A, A') or 10μM forskolin (C, C'). Graphs show quantification of FRET/CFP fluorescence intensity in representative cells upon treatment with isoproterenol (B) or forskolin (D), which revealed a 1.14-fold and 1.45-fold increase in PKA activity in response to these agonists, respectively. This activation reached its peak within just 2 mins of treatment. (E) Western blot analysis of cell lysates from primary rat hepatocytes shows a substantial increase in the number and intensity of PKA-phosphorylated substrates following 24 h stimulation with 50μM isoproterenol or 10μM forskolin + 0.5mM IBMX.

Figure 3: *Lipolysis is activated in hepatocytes by isoproterenol.* (A) Confocal images of ORO-stained LDs and corresponding graph show a significant ~40% reduction in LD area/cell following 24 h treatment with isoproterenol (50μM). (B) In contrast, isoproterenol had no effect on LD content in the presence of the PKA inhibitor H89 (10μM). In addition, inhibition of lipolysis by the ATGL inhibitor atglistatin (C, 10μM) or the HSL inhibitor CAY10499 (D, 10μM) also inhibited isoproterenol-mediated LD loss. (E) Western blot analyses revealed β-AR/cAMP-stimulated HSL phosphorylation (S660) in primary rat hepatocytes and ATGL phosphorylation (S404) in Hep3B cells (F), both of which were inhibited by H89. Dashed circles denote nuclei position in confocal images. Statistical analysis of fold change was done using a two-tailed paired T-test; ** denotes $n<0.01$.

Figure 4: *Stimulated recruitment of ATGL to hepatocellular LDs by cAMP elevation.* (A) Western blot analysis of isolated LDs and post-nuclear supernatant (PNS) from HuH-7 cells treated with 0.1% DMSO or 10μM forskolin for 1 h. (B) Corresponding graph shows quantification of ATGL/Plin2 from isolated LDs (n=3, mean ± SD, $p<0.05$). (C) Fluorescent images show Hep3B cells expressing ATGL(S47A)-EGFP and co-labeled with the LD marker MDH (red). Note the increase in EGFP intensity around the LDs following isoproterenol treatment (50μM, 60 min), quantified in (D) (n=10 cells from 3 independent experiments; *$p<0.05$). (E) Heatmap of ATGL intensity shows a substantial reduction in cytosolic fluorescence (yellow arrows) and corresponding increase in fluorescence around the LD periphery. (F-H) Images and corresponding graph show 60-minute treatment with forskolin also causes ATGL recruitment to the LD which is blocked by pre-treatment with 10μM H89. (n=13-14 cells from 3 independent experiments; *$p<0.05$) Statistical analysis of fold change was done using a two-tailed paired T-test; * denotes $n<0.05$; ** denotes $n<0.01$.

Figure 5: *Hormone-sensitive lipase (HSL) is recruited to hepatocyte LDs in response to cAMP agonists.* (A) Fluorescent images of Hep3B cells expressing HSL-sfGFP and labeled with the LD marker MDH (red) show an increase in LD-localized sfGFP intensity following isoproterenol treatment (50μM, 30min), which is quantified in (B) (n=13 cells from 3 independent experiments; *$p<0.05$). (C-E) Fluorescent images and the corresponding graph show treatment with forskolin also causes HSL recruitment to the LD, a response that is blocked by pre-treatment with 10μM H89. (n=13-19 cells from 3 independent

experiments; *p<0.05) Statistical analysis of fold change was done using a two-tailed paired T-test; * denotes n<0.05.

Figure 6: *Fluorescence Recovery After Photobleaching (FRAP) of cytosolic lipases ATGL and HSL is inhibited by H89.* (A) A temporal sequence of fluorescence images from individual LDs within Hep3B cells expressing ATGL(S47A)-EGFP. Fluorescence Recovery after Photobleaching (FRAP) was measured on ATGL localized around LDs in live cells in the presence and absence of the PKA inhibitor H89 (10μM). Following photobleaching, ATGL recovered steadily over the course of 20 minutes (representing lipase exchange on the LD surface) while virtually no FRAP was observed around LDs in cells pre-treated with H89. (B) Line graph of FRAP over time and (C) quantification of fold recovery for ATGL(S47A)-EGFP confirms a significant inhibition by H89 (n=8-10 cells from 3 independent experiments). The same FRAP approach was performed on HSL-sfGFP around LDs in the presence and absence of H89 (D), quantified over time as % FRAP (E) and fold recovery (G) (n=9-12 cells from 3 independent experiments). The FRAP exchange of HSL-sfGFP was also attenuated by pre-treatment with H89, although to a lesser extent than that of ATGL. (G) The rate of recovery for each lipase was also quantitated, showing a 5-fold slower recovery by ATGL vs. HSL. Statistical analysis was done using a two-tailed Students T-test.

Figure 7: *EtOH exposure inhibits hepatocellular lipolysis.* (A) Confocal micrographs of ORO-stained LDs in primary hepatocytes isolated from rats that were fed a chronic EtOH diet or an isocaloric control diet for 6 weeks. Cells were treated with 50μM isoproterenol or 10μM forskolin + 0.5mM IBMX for 24 hours. (B) Quantification of fold change in LD area/cell shows a significant reduction in control hepatocytes, but no agonist-induced decrease in hepatocytes from chronic EtOH-fed rats. (C) Triglyceride efflux measurements from primary hepatocytes isolated from pair-fed control vs chronic EtOH-fed rats also show a significant inhibition by chronic EtOH exposure on cells treated with Fsk+IBMX, and total TG efflux is blocked by the lipase inhibitor atglistatin. (D-E) Western blot analysis of primary hepatocyte lysates show cAMP/PKA-dependent phosphorylation of HSL was diminished 3-fold in hepatocytes isolated from chronic EtOH-fed rats as confirmed by densitometry quantification. (F) Western blot analysis of adenylate cyclase 3 and PKA-Cα revealed no significant change in protein levels between hepatocytes from control vs chronic EtOH-fed rats. (G) Western blot analysis of primary hepatocytes from control vs EtOH-fed rats (C vs E) treated for 1 hour with 8-Br-cAMP (10μM, 100μM) or with Fsk+IBMX reveals a reduction in PKA substrates and phospho-HSL (S660). Densitometry quantification shows a 60-80% reduction in PKA substrate phosphorylation (H) and a ~90% reduction in HSL phosphorylation (I). All data represent three independent experiments. Error bars denote standard deviation. Asterisks denote statistical significance as measured by student's T-test (*p<0.05; **p<0.01). Dashed circles denote nuclei position in confocal images.

Figure 8: *Ethanol inhibits ATGL recruitment and PKA activation in VA-13 hepatocytes*. (A) VA-13 cells were cultured for 48 hours in the presence or absence of 50mM EtOH and transfected with the lipase inactive ATGL(S47A)-EGFP to measure lipase trafficking to the LD. Representative images show 10μM isoproterenol + 0.5mM IBMX induced the recruitment of ATGL to the LD following 30 minutes under control conditions, but this recruitment was not observed in cells exposed to EtOH. (B) Quantification of the fold increase in ATGL intensity around the LD relative to cytosolic fluorescence intensity following isoproterenol treatment (50μM; 30 min; n=9-13 cells from 3 separate experiments). (C) Western blot analysis confirms the overexpression of ADH in VA-13 cells, and not their derivative cell line, HepG2. (D) Representative Western blot showing diminished phosphorylation of PKA substrates phosphorylation of total substrate proteins in VA-13 cells following multi-day incubation in 50mM EtOH. (E) Quantification of PKA substrates by densitometry revealed a significant ~30% decrease in PKA activity by day 2 and a ~50% reduction by day 5. (n=3 experiments) Error bars denote standard deviation. Statistical analysis of fold change was done using a two-tailed paired T-test.

Figure 1 (Revised)

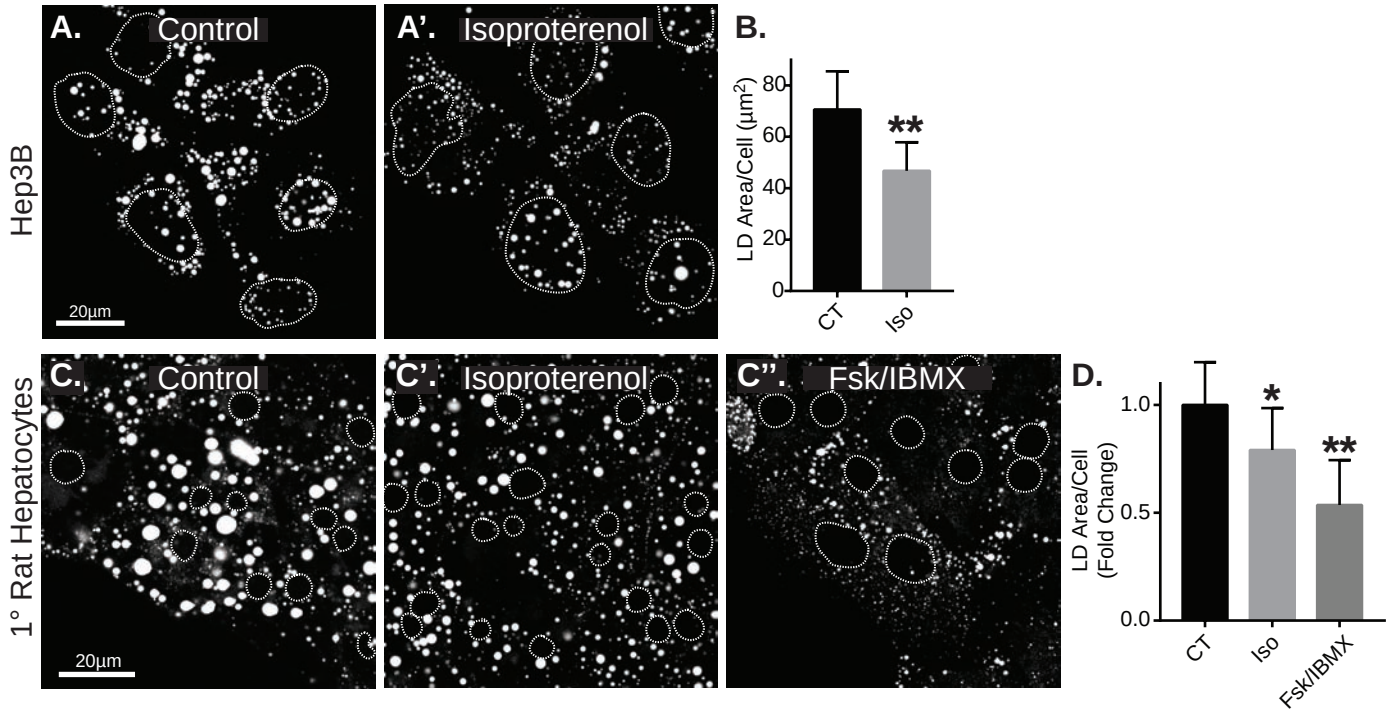

Figure 2 (2-column width)

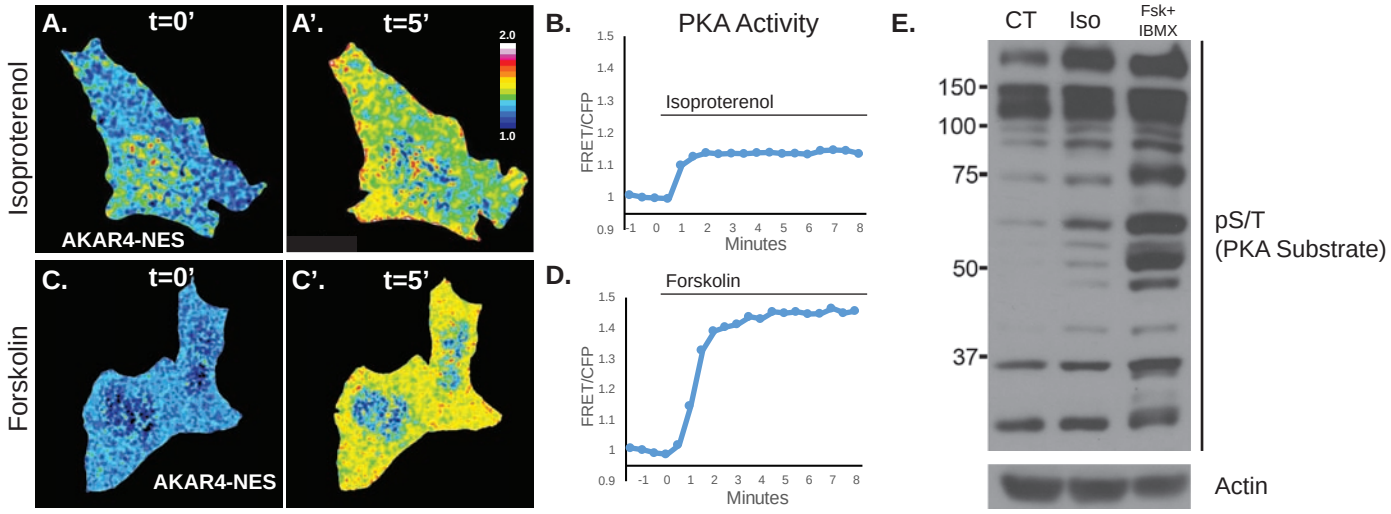

Figure 3 (Revised)

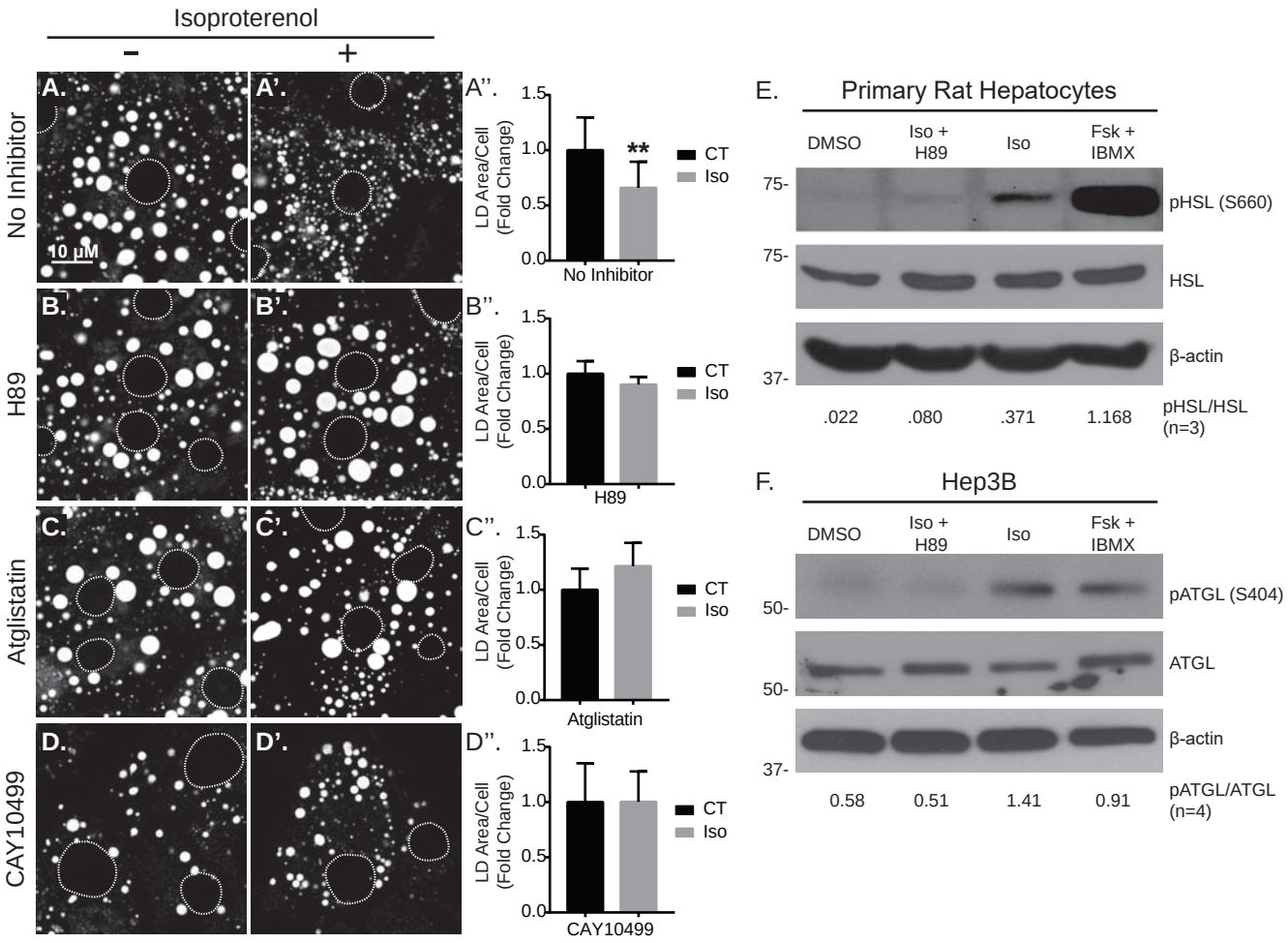

Figure 4 (Revised)

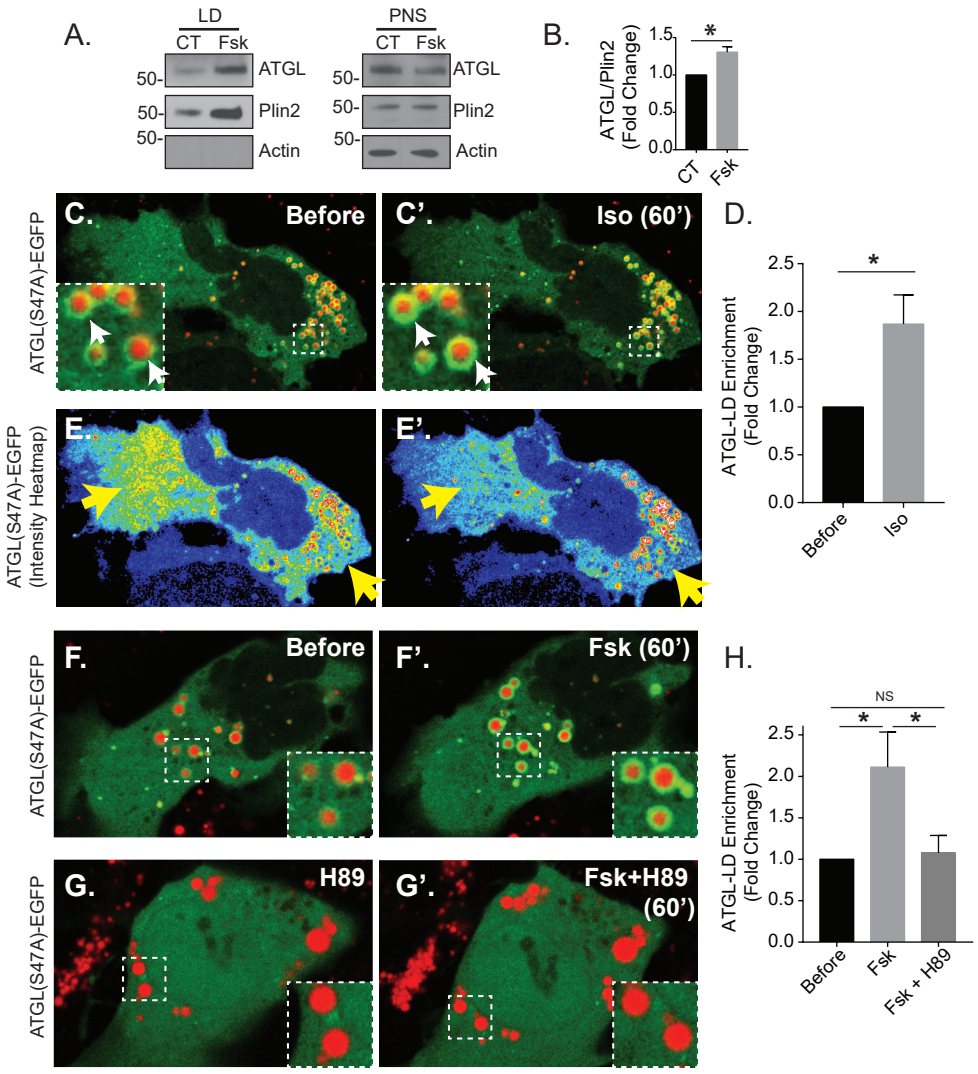

Figure 5 (1.5-column width)

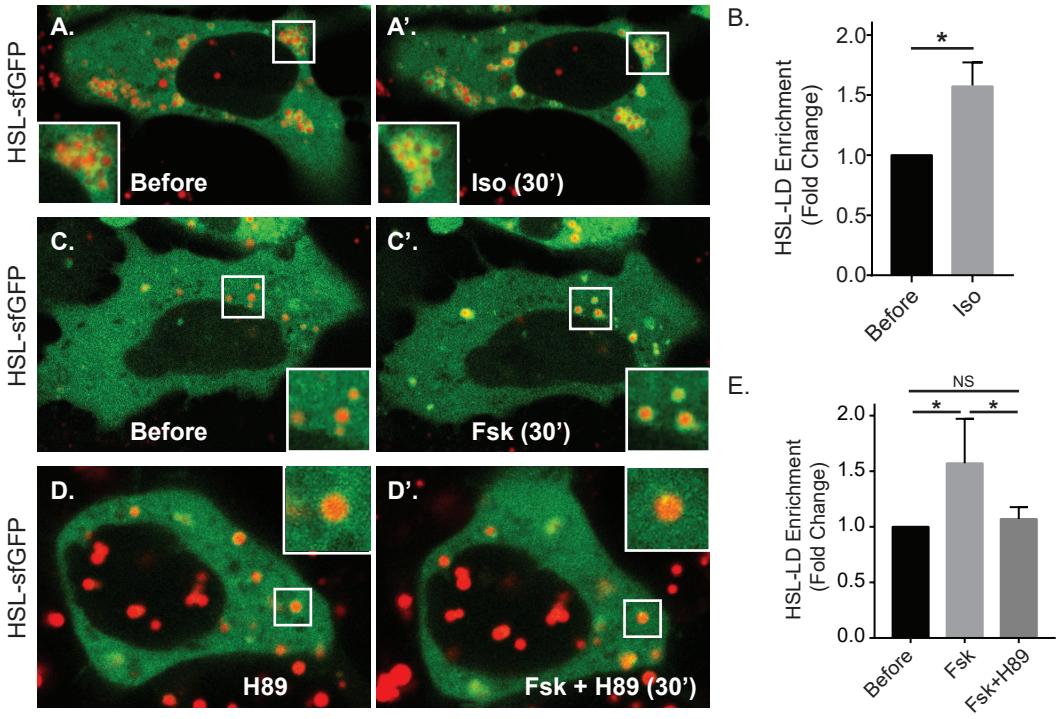

Figure 6 (2-column width)

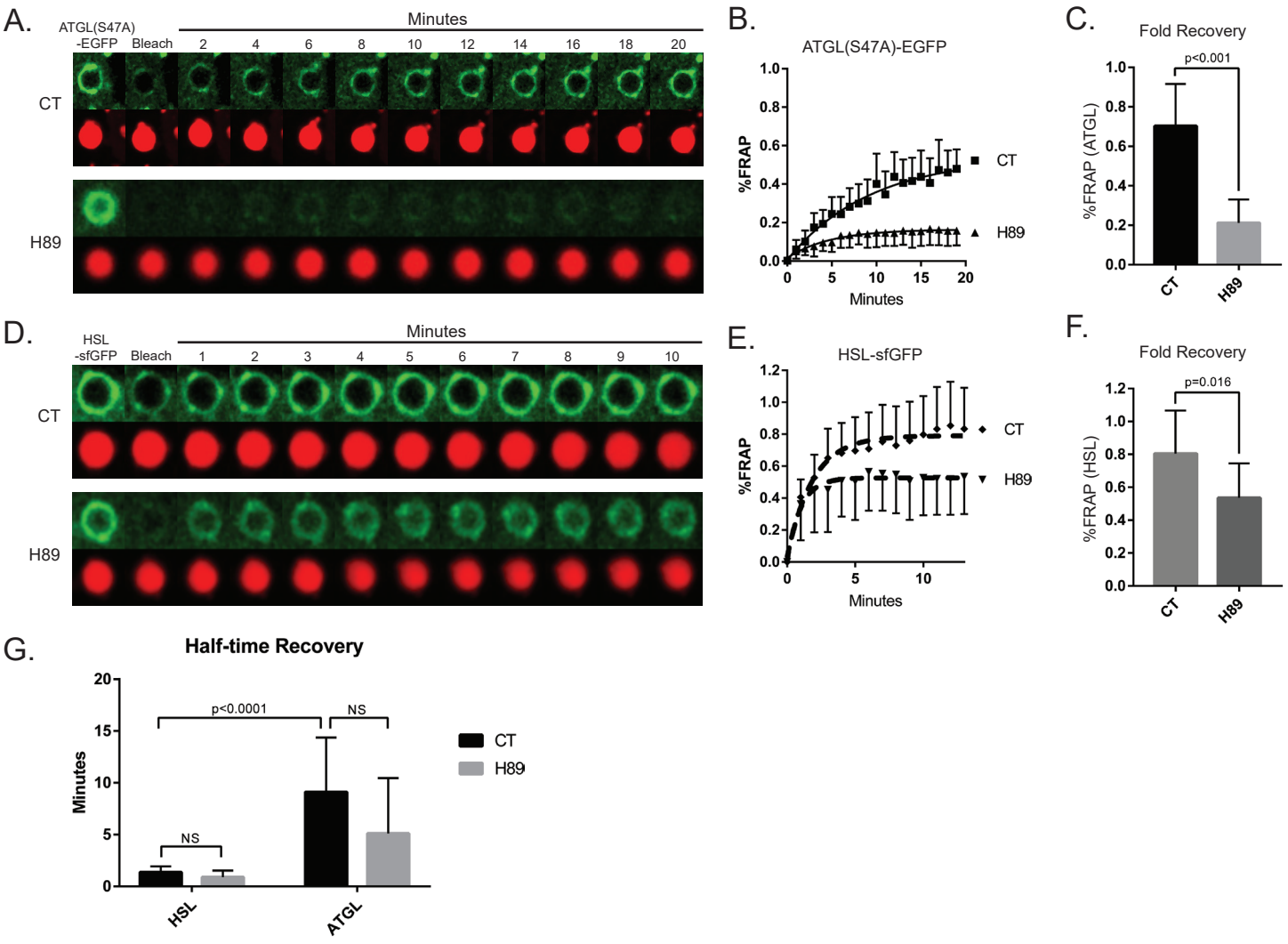

Figure 7 (revised)

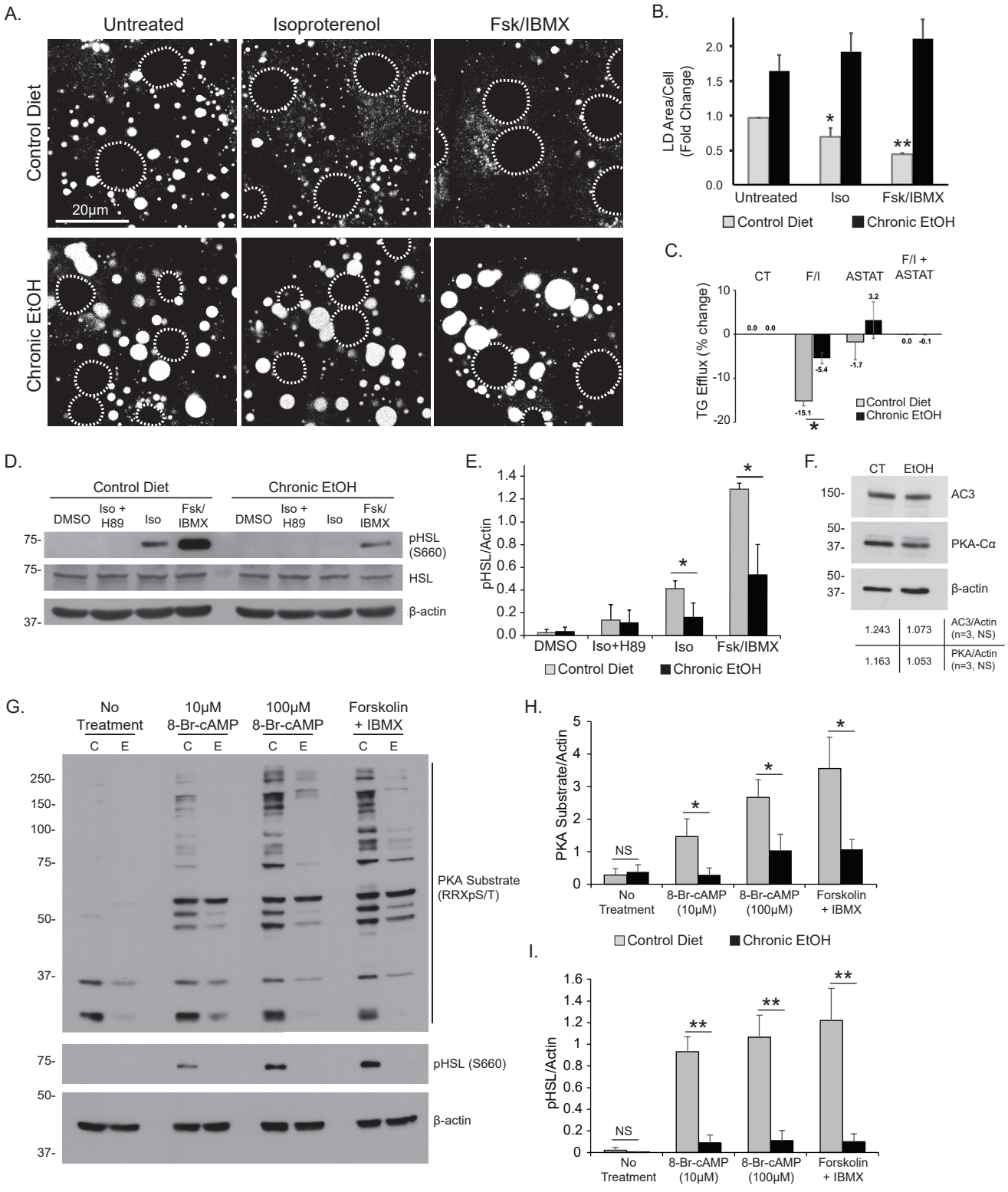

Figure 8 (Revised)

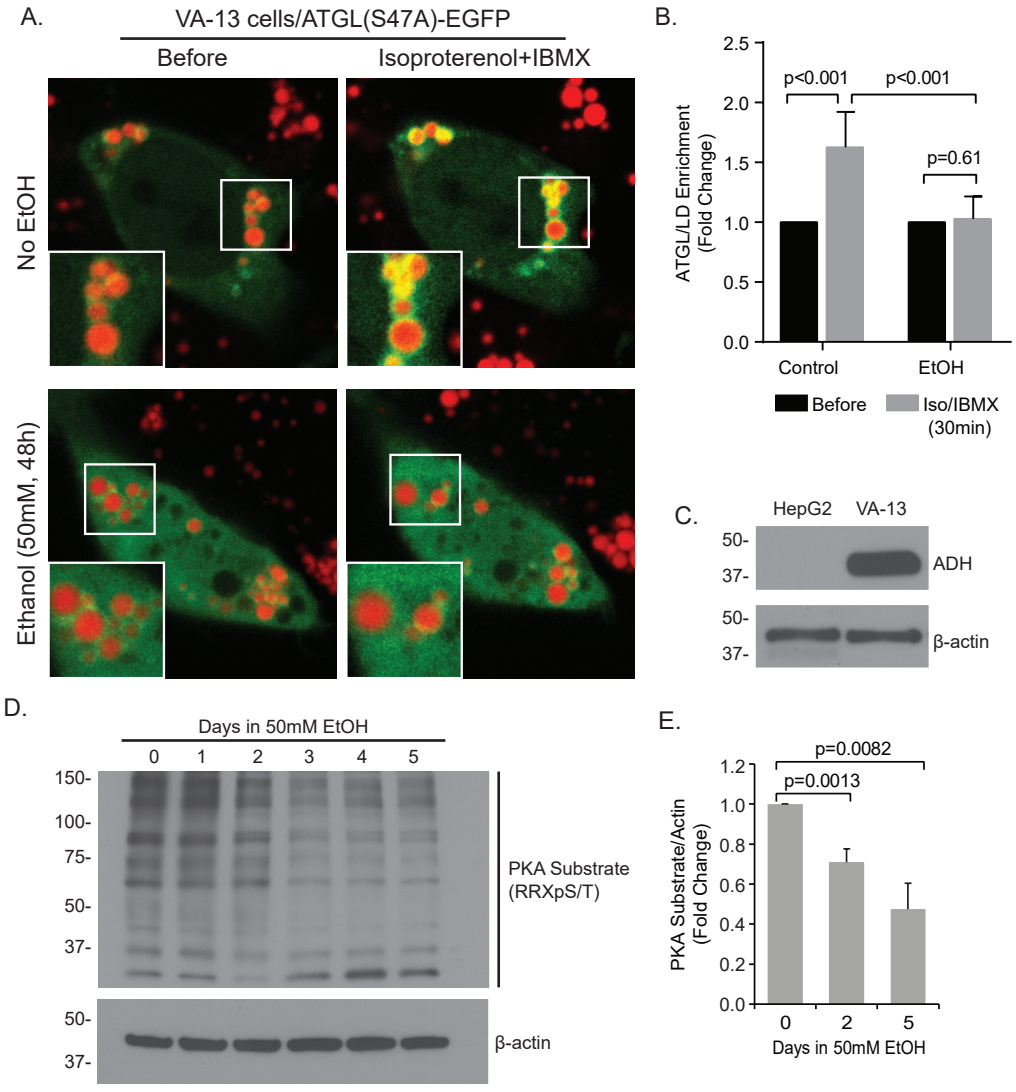

β-adrenergic induction of lipolysis in hepatocytes is inhibited by ethanol exposure

Micah B. Schott, Karuna Rasineni, Shaun G. Weller, Ryan J. Schulze, Arthur C. Sletten, Carol A. Casey and Mark A. McNiven

J. Biol. Chem. published online May 17, 2017